Toxicological interactions of perfluorooctane sulfonic acid (PFOS) and perfluorooctanoic acid (PFOA) with selected pollutants

Ismael Rodea-Palomares [a], Francisco Leganés [a], Roberto Rosal [b], Francisca Fernández-Piñas [a,*]

[a] Departamento de Biología, Facultad de Ciencias, Universidad Autónoma de Madrid, Cantoblanco, 28049 Madrid, Spain
[b] Departamento de Ingeniería Química, Universidad de Alcalá, E-28871, Alcalá de Henares, Madrid, Spain

ARTICLE INFO

ABSTRACT

The combined toxicity of the perfluorinated surfactants perfluorooctane sulfonic acid (PFOS), perfluorooctanoic acid (PFOA) and several pollutants (Hg^{2+}, Cd^{2+}, 2,4-D, propylparaben, mitomycin C and furazolidone) has been examined with a bioluminescent cyanobacterial toxicity test. Hg^{2+}, Cd^{2+}, mitomycin C and furazolidone could be included in the "Acute aquatic hazard" category established in the Regulation (EC) No 1272/2008 being "very toxic to aquatic life". Toxicological interactions of PFOA, PFOS with these pollutants in binary, ternary and multicomponent mixtures were studied using the combination-index method. PFOA and PFOS showed an antagonistic interaction at the whole range of effect levels, this may explain in part the finding that PFOA and PFOS interacted in an inverse way with the organic pollutants; the relative hydrophobicity of the tested compounds would also explain this interaction pattern. The interaction of both PFOS and PFOA with heavy metals was mostly antagonistic, decreasing metal toxicity. With increasing complexity of the mixtures, the CI method predicted synergism at low to very low levels of effect; pollutant combinations at their mixture NOECs were tested and confirmed the predicted synergism.

© 2011 Elsevier B.V. All rights reserved.

1. Introduction

Surfactants are synthetic chemicals used in large amounts in a variety of industrial cleansing processes as well as in consumer products. Perfluorinated chemicals (PFCs) are synthetic fluorinated surfactants composed of a carbon backbone and a charged functional group. The eight-carbon backbone perfluorooctane sulfonic acid (PFOS) and perfluorooctanoic acid (PFOA) are two of the most widely used PFCs. The strong covalent bond between the fluor and carbon ions makes PFCs thermally and chemically stable; they are also oil and water repellent; these unique properties make these chemicals highly resistant to both chemical and biological degradation under normal environmental conditions and have been found to be highly persistent in the environment [1–3]. Their global occurrence, persistence in the environment and bioaccumulation in biota has increased the concerns about possible toxic effect of PFCs. In 2000, the US-EPA declared PFOS and PFOA withdrawal to avoid environmental pollution and potential health risks; the OECD in 2000 declared these substances as biopersistent, bioaccumulative and toxic to mammals; PFOS was finally banned in Europe by the directive 2006/122/EC and recently added to the Annex B of the Stockholm Convention on Persistent Organic Pollutants.

Due to the bioaccumulation of PFCs in humans and associated potential toxicity, most toxicological studies have been made in rodents and/or human cell lines; however, there is comparatively less information on the ecotoxicity of these chemicals in the aquatic environment. In addition, in the aquatic environment, various PFCs co-exist and co-occur with a variety of other xenobiotics [4–6]; thus, to obtain a full picture of the true impact of PFCs, studies on aquatic toxicity of representative PFCs such as PFOS and PFOA applied singly and in combination as well as combined with other xenobiotics are needed. Chemicals in a complex mixture may either not interact or synergistically or antagonistically interact [7–10]; interactions which should be taken into account when considering risk assessment strategies. There are very few reports on the interaction between PFOA and PFOS themselves or on the interactions of PFOA and PFOS with other xenobiotics which is of special concern considering the ability of PFCs to solubilize non-polar compounds [11]. Most of these interaction studies have been performed with PFOS [12–15]; to our knowledge, no previous studies about toxicological interactions of PFOA with other xenobiotics have been reported.

The aim of this study was to assess the nature of the interactions between PFOS and PFOA as well as PFOS and/or PFOA combined with selected priority and emerging pollutants. As

* Corresponding author. Tel.: +34 914978176; fax: +34 914978344.
  E-mail address: francisca.pina@uam.es (F. Fernández-Piñas).

toxicity endpoint we have chosen the bioluminescent response of the recombinant bioluminescent cyanobacterium *Anabaena* CPB4337 [8,16,17]. Cyanobacteria are a relevant and abundant group of primary producers (dominant in some aquatic and terrestrial ecosystems) which are prokaryotic in nature and are at the very base of the trophic webs. Furthermore, some species such as this *Anabaena* strain can fix atmospheric nitrogen into bioavailable forms, ability which being only prokaryotic is not shared with green algae and plants so that they are an important source of bioavailable nitrogen for many ecosystems (especially in oligotrophic aquatic ecosystems [18]). Cyanobacteria provide the biofuels needed by many other organisms and any detrimental effect on this group may have a negative impact in nutrient availability to organisms of higher trophic levels. In order to identify and quantify the nature of the interactions between the fluorinated surfactants and the pollutants, we made binary, ternary and complex mixtures of these pollutants with PFOS and PFOA which were analyzed by the method of the combination index (CI)-isobologram equation which we have previously used to study the combined effects of pollutant mixtures [8,9].

2. Material and methods

2.1. Materials

PFOS (98%) was obtained from Fluka, PFOA (96%), mitomycin C (MMC) (97%), Hg²⁺ (as HgCl₂) (99%) and Cd²⁺ (as CdCl₂) (97.5%) were purchased from Sigma–Aldrich. Propyl 4-hydroxybenzoate (propylparaben; PPB), 2-(2,4-dichlorophenoxi) acetic acid (2,4-D) and 3-{[(5-nitro-2-furyl)methylene]amino}-1,3-oxazolidin-2-one (furazolidone; FURA) (98%) were obtained from Alfa Aesar. CAS No, molecular formula and main physicochemical properties of these compounds are summarized in Table 1, $\log K_{ow}$ and $\log D_{ow}$ are included as descriptors of the hydrophobicity of the tested chemicals. Polar surface area (PSA) is included as a descriptor of passive molecular transport through membranes [19].

We avoided the use of solvents when possible, with the only exceptions of the stock solutions of mitomycin C which was prepared in methanol, and 2,4-D and furazolidone, which were prepared in DMSO. Final concentrations of methanol and DMSO in the assay medium were always below 0.005% (v/v). No significant effect on bioluminescence of *Anabaena* CPB 4337 was found for these concentrations of solvents (not shown). Stock solutions and dilutions used in the bioassays were stored in the dark at −20 °C.

2.2. Toxicity bioassays

The bioassays using the recombinant bioluminescent cyanobacterium *Anabaena* CPB4337 were based on the inhibition of constitutive luminescence caused by the presence of any toxic substance and were performed as previously described [16,17,20]. The stability of target compounds under the bioassay conditions was examined according to OECD Guidance [21]. Analyses have been performed at the start and at the end of the 24 h-exposure test for the highest concentration and for a concentration near the EC₅₀ (D_m) using an HPLC–diode array liquid chromatograph or ICP-MS, except for those for which stability was previously assessed [9]. HPLC analyses were performed using a Hewlett Packard 1200 Series device (Agilent Technologies, Palo Alto, CA, USA) equipped with a reversed phase Kromasil 5u 100A C18 analytical column. The mobile phase was a mixture of acrylonitrile (50%) and acidified water (50%). UV detection was carried out at 230 nm (MMC), 360 nm (FURA), 254 nm (PPB) and 360 nm (2,4-D). Inductively coupled plasma-mass spectrometry analyses were used to determine the exposure concentration of mercury and cadmium. The

Table 1
Physicochemical properties of Hg²⁺ (as HgCl₂) (Hg), Cd²⁺ (Cd), propyl 4-hydroxybenzoate (Propylparaben, PPB) (2,4-dichlorophenoxy) acetic acid (2,4-D), furazolidone (FURA), mitomycin C (MMC), perfluorooctanoic acid (PFOA) and perfluorooctane sulfonic acid (PFOS).
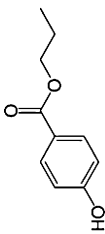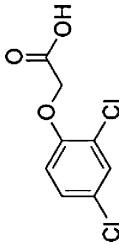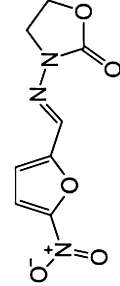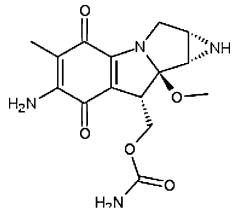
Compound	CAS No.	Molecular structure	Molecular weight (g/mol)	Water Solubility (g/l)	pKₐ	Log K_{ow} [a]	Log D_{ow} [b]	PSA[c] (Å²)
Hg²⁺ (as HgCl₂)	7487-94-7	–	271.52	74	–	3.2	3.2	–
Cd²⁺ (as CdCl₂)		–	183.32	1350	–	−0.07	−0.07	–
propyl 4-hydroxybenzoate (Propylparaben, PPB)	94-13-3		180.2	1.1	8.23	2.901	2.90	46.5
(2,4-Dichlorophenoxy) acetic acid (2,4-D)	94-75-7		221.04	367	2.98	2.426	−0.59	46.5
3-{[(5-nitro-2-furyl)methylene]amino}-1,3-oxazolidin-2-one (Furazolidone, FURA)	67-45-8		225.158	0.12	−1.98	−0.050	−0.05	101

Table 1 (*Continued*)
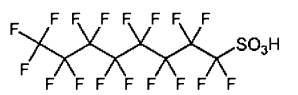
Compound	CAS No.	Molecular structure	Molecular weight (g/mol)	Water Solubility (g/l)	pK_a	Log K_{ow}[a]	Log D_{ow}[b]	PSA[c] (Å^2)
Mitomycin C	50-07-7		334.33	0.57	13.27	−0.298	−0.30	147
Perfluorooctanoic acid (PFOA)	335-67-1		414.07	13.6	0.50	6.444	0.94	37.3
Perfluorooctane sulfonic acid (PFOS)	1763-23-1		500.13	7.5	−3.27	4.512	−4.76	62.8

[a] Log K_{ow} (log P) = log of octanol–water partition coefficient.

[b] Log D_{ow} = The octanol–water partition coefficient, K_{ow}, is a measure of the hydrophobicity of a given neutral compound. For compounds that dissociate in aqueous solution, the corresponding acid–base equilibrium has to be considered originating an apparent octanol–water partition coefficient, usually represented D_{ow}. For the computation of D_{ow}, both pH and the dissociation constant of acidic of basic compounds, pK_a are required. For acidic compounds, the Herderson–Hasselbalch equations yield:

$$D_{ow} = \frac{K_{ow}}{1 + 10^{pH - pK_a}} \tag{1}$$

For basic drugs, the apparent partition coefficient can be expressed by means of the pK_a for their conjugate acids:

$$D_{ow} = \frac{K_{ow}}{1 + 10^{pK_a - pH}} \tag{2}$$

For neutral substances,

$$D_{ow} = K_{ow}. \tag{3}$$

[3].

[c] PSA = Polar surface area: The polar surface area (PSA) is defined as the surface overall sum of polar atoms (usually oxygen and nitrogen), including also attached hydrogens.
PSA is a commonly used medicinal chemistry metric for the optimization of cell permeability. Molecules with a polar surface area of greater than 140 Å^2 are usually believed to be poor at permeating cell membranes [19].

equipment used was a quadrupole mass spectrometer Agilent 7700X operating at 3 MHz in helium cell gas mode. No significant differences were found between the nominal and measured exposure concentrations for Hg^{2+}, Cd^{2+}, 2,4-D, PPB, PFOA and PFOS; thus, throughout the present study, their nominal concentrations were used for data analyses. In the case of MMC and FURA, the final concentration/initial concentration ratios (in abiotic conditions) were 0.038 for MMC and 0.73 for FURA. In both cases, for data analyses, exposure concentrations were used instead of nominal concentrations according to OECD Guidance (OECD, 2008).

2.3. Experimental design of PFOS/PFOA/selected chemicals combinations

Solutions of PFOS, PFOA, $HgCl_2$, $CdCl_2$, propylparaben, 2,4-D, furazolidone and mitomycin C were used singly and in the binary, ternary and multicomponent mixtures shown in Table 2. Anabaena cells were treated with serial dilutions of each chemical individually and with a fixed constant ratio (1:1), based on the individual EC_{50} values, in their combinations. Five to seven dilutions (serial dilution factor = 2) of each chemical and combination plus a control were tested in three independent experiments with replicate samples as described elsewhere [8].

2.4. Median-Effect and combination index (CI)-isobologram equations for determining individual and combined toxicities

The response to toxic exposure in Anabaena CPB4337 test was estimated using the median-effect equation based on the mass-action law [22]:

$$\frac{f_a}{f_u} = \left(\frac{D}{D_m}\right)^m \tag{1}$$

where D is the dose, D_m is the dose for 50% effect (EC_{50}), f_a is the fraction affected by dose D (e.g., 0.75 if cell bioluminescence is inhibited by 75%), f_u is the unaffected fraction (therefore, $f_a = 1 - f_u$), and m is the coefficient of the sigmoidicity of the dose–effect curve: $m = 1$, $m > 1$, and $m < 1$ indicate hyperbolic, sigmoidal, and flat sigmoidal dose–effect curve, respectively. Therefore, the method takes into account both the potency (D_m) and shape (m) parameters. If Eq. (1) is rearranged, then:

$$D = D_m \left[\frac{f_a}{(1-f_a)}\right]^{1/m} \tag{2}$$

The D_m and m values for each individual compound or mixture were determined by the median-effect plot: $x = \log(D)$ versus $y = \log(f_a/f_u)$ which is based on the logarithmic form of Eq. (1). In the median-effect plot, m is the slope and $D_m = 10^{-(y-\text{intercept})/m}$. The conformity of the data to the median-effect principle can be ready manifested by the linear correlation coefficient (r) of the data to the logarithmic form of Eq. (1) [23].

These parameters were then used to calculate doses of individual compounds and their mixtures required to produce various effect levels according to equation 1; for each effect level, combination index (CI) values were then calculated according to the general combination index equation for n-chemical combination at x% inhibition [23]:

$$^n(CI)_x = \sum_{j=1}^{n} \frac{(D)_j}{(D_x)_j} = \sum_{j=1}^{n} \frac{(D_x)_{1-n}\left\{[D]_j / \sum_1^n [D]\right\}}{(D_m)_j \left\{(f_{ax})_j / [1-(f_{ax})_j]\right\}^{1/mj}} \tag{3}$$

where $^n(CI)_x$ is the combination index for n chemicals at x% inhibition; $(D_x)_{1-n}$ is the sum of the dose of n chemicals that exerts x% inhibition in combination, $\left\{[D]_j / \sum_1^n [D]\right\}$ is the proportionality of the dose of each of n chemicals that exerts x% inhibition in combination; and $(D_m)_j\{(f_{ax})_j / [1-(f_{ax})_j]\}^{1/mj}$ is the dose of each drug

alone that exerts x% inhibition. From Eq. (3), CI < 1, CI = 1 and CI > 1 indicates synergism, additive effect and antagonism, respectively.

2.5. Analysis of results

Computer program CompuSyn [24] was used for calculation of the individual and combined dose–effect curve parameters; CI values of the different mixtures; f_a–CI plots and polygonograms. Linear regression analyses were computed using MINITAB Release 14 for Windows (Minitab Inc; USA). The mixture NOECs (no observed effect concentrations) were determined by Dunnett's multiple comparison procedure [25,26] ($p \leq 0.05$) using also Minitab.

3. Results

3.1. Toxicity of individual compounds

Table 2 shows the dose–effect curve parameters (D_m, m and r) of the eight compounds tested in this study using the Anabaena CPB4337 24-h toxicity test singly and in their binary, ternary and multi-component mixtures (6–8 components); 95% confidence intervals are indicated for the D_m and m parameters. For single components, D_m (EC_{50}) in mg/l were as follows: MMC (0.014), Hg (0.070), Cd (0.091), FURA (0.974), 2,4-D (3.74), PPB (11.91), PFOS (16.29) and PFOA (19.81). D_m values of MMC, Hg^{2+} and Cd^{2+} were the lowest, and could be included in the "Acute aquatic hazard" category established in the Regulation (EC) No. 1272/2008 ($EC_{50} < 1$ mg/l) and classified as "very toxic to aquatic life" (H400); although FURA, strictly according to its D_m value, could also be classified as very toxic, confidence intervals do not exclude a lower toxicity of this compound.

3.2. Toxicological interactions of PFOA and PFOS with selected pollutants in binary and ternary combinations in the Anabaena CPB4337 bioluminescence test

Fig. 1 shows the f_a–CI plots of binary and ternary mixtures for the Anabaena tests. The f_a–CI plot depicts the CI value versus f_a (the effect level or fraction of luminescence inhibited with respect to the control). Average CI values for three representative effect levels (EC_{10}, EC_{50} and EC_{90}) are also shown in Table 2.

Fig. 1a and b shows the f_a–CI plots for PFOA/PFOS/Heavy metals binary and ternary combinations. The $Hg^{2+} + Cd^{2+}$ combination showed a slight antagonism in almost the whole range of effect levels, approaching an additive effect at the highest f_a values. Regarding PFOA/heavy metals mixtures (Fig. 1a), the PFOA + Hg^{2+} combination showed a strong antagonism in the f_a range; the PFOA + Cd^{2+} combination was also antagonistic but to a lesser degree than the PFOA + Hg^{2+} combination.

The ternary mixture PFOA + Hg^{2+} + Cd^{2+} led to dual synergistic/antagonistic behavior being synergistic at f_a values below 0.2, additive at f_a values between 0.2 and 0.4, and turning into antagonism at f_a values above 0.4.

Correlation analyses were made between CI values of the ternary combinations and CI values of each of the binary combinations to determine which binary combination was predominant in the ternary mixture (Table 3). In this correlation analysis, for the ternary mixture PFOA + Hg^{2+} + Cd^{2+}, the highest correlation coefficient was found for the PFOA + Cd^{2+} combination ($r = 0.988$), suggesting that this combination interaction predominated in the three compound mixture.

In the PFOS–heavy metal mixtures (Fig. 1b), binary combinations of PFOS + Hg^{2+} and PFOS + Cd^{2+} also showed a strong antagonism in the whole range of effect levels (f_a), but with a tendency of increasing antagonism in the case of PFOS + Cd^{2+} while in the PFOS + Hg combination, there was

Table 2

Dose–effect relationship parameters (indicating 95% confidence intervals) and mean combination index (CI) values of Hg, Cd, PPB, 2,4-D, FURA, MMC, PFOA and PFOS, individually and of their binary, ternary and multicomponent (six or more components) combinations on *Anabaena* CPB4337 bioluminescence test.

Drug combo	Dose–effect parameters			CI Values at					
	D_m	m	r	EC_{10}		EC_{50}		EC_{90}	
Hg	0.070 (0.04–0.1)	2.618 (1.83–3.32)	0.960	–		–		–	
Cd	0.091 (0.06–1.116)	2.321 (1.88–2.75)	0.935	–		–		–	
PPB	11.91 (5.32–18.39)	2.198 (1.53–2.86)	0.916	–		–		–	
2,4-D	3.740 (1.24–6.89)	2.606 (1.83–3.37)	0.933	–		–		–	
FURA	0.974 (0.25–1.69)	2.399 (1.39–3.40)	0.949	–		–		–	
MMC	0.014 (0.006–0.02)	2.654 (2.02–3.12)	0.912	–		–		–	
PFOA	19.81 (15.44–26.44)	2.122 (1.97–2.66)	0.950	–		–		–	
PFOS	16.29 (10.04–23.85)	1.805 (1.35–2.27)	0.884	–		–		–	
Binary mixtures									
Hg + Cd	0.111 (0.04–0.178)	2.556 (1.63–3.47)	0.953	1.38 ± 0.07	Ant	1.30 ± 0.03	Ant	1.22 ± 0.02	Ant
2,4-D + PPB	2.720 (1.41–3.01)	1.618 (1.07–2.15)	0.925	0.33 ± 0.03	Syn	0.54 ± 0.03	Syn	0.88 ± 0.03	Syn
MMC + FURA	0.210 (0.121–0.310)	1.985 (1.02–2.25)	0.938	0.54 ± 0.03	Syn	0.69 ± 0.03	Syn	0.89 ± 0.05	Syn
PFOA + PFOS	93.85 (66.96–110.5)	3.367 (2.04–5.56)	0.923	4.18 ± 0.73	Ant	3.77 ± 0.34	Ant	3.41 ± 0.25	Ant
PFOA + Hg	41.15 (36.22–55.12)	2.386 (1.30–3.46)	0.900	3.09 ± 0.10	Ant	2.91 ± 0.11	Ant	2.75 ± 0.11	Ant
PFOA + Cd	13.20 (6.32–17.21)	2.026 (1.49–2.57)	0.939	1.34 ± 0.04	Ant	1.48 ± 0.03	Ant	1.64 ± 0.06	Ant
PFOA + PPB	11.45 (8.23–16.45)	1.221 (0.73–1.47)	0.928	0.31 ± 0.01	Syn	0.69 ± 0.01	Syn	1.50 ± 0.08	Ant
PFOA + 2,4-D	10.05 (7.10–17.23)	2.117 (1.45–2.67)	0.918	1.21 ± 0.07	Ant	1.41 ± 0.03	Ant	1.65 ± 0.06	Ant
PFOA + FURA	27.04 (10.56–35.39)	2.717 (1.34–3.58)	0.878	3.42 ± 0.23	Ant	2.91 ± 0.11	Ant	2.49 ± 0.15	Ant
PFOA + MMC	4.695 (3.23–5.66)	1.841 (1.03–2.66)	0.921	0.68 ± 0.04	Syn	0.93 ± 0.04	Add	1.28 ± 0.13	Ant
PFOS + Hg	60.52 (52.98–76.42)	3.356 (2.78–4.67)	0.903	7.20 ± 1.54	Ant	4.28 ± 0.40	Ant	2.59 ± 0.22	Ant
PFOS + Cd	58.00 (43.52–62.56)	1.119 (0.75–1.75)	0.946	2.29 ± 0.12	Ant	5.24 ± 0.17	Ant	12.1 ± 0.66	Ant
PFOS + 2,4-D	6.787 (2.34–10.65)	2.568 (1.97–2.84)	0.949	0.89 ± 0.08	Add	0.76 ± 0.03	Syn	0.67 ± 0.02	Syn
PFOS + PPB	53.14 (43.34–65.68)	1.699 (1.12–1.99)	0.938	3.07 ± 0.17	Ant	3.46 ± 0.10	Ant	3.93 ± 0.15	Ant
PFOS + FURA	9.955 (4.92–14.99)	2.215 (1.49–3.26)	0.928	1.01 ± 0.07	Add	0.88 ± 0.03	Add	0.78 ± 0.06	Syn
PFOS + MMC	6.360 (5.67–9.10)	3.490 (2.44–3.89)	0.946	1.24 ± 0.02	Ant	0.83 ± 0.01	Syn	0.58 ± 0.03	Syn
% of Synergistic mixtures					25%		31%		31%
Ternary mixtures									
PFOA + Hg + Cd	8.717 (6.52–12.55)	1.560 (0.87–1.76)	0.921	0.74 ± 0.03	Syn	1.15 ± 0.03	Ant	1.80 ± 0.12	Ant
PFOA + 2,4-D + PPB	7.317 (3.87–12.71)	3.210 (1.94–5.68)	0.935	1.17 ± 0.03	Ant	0.94 ± 0.01	Syn	0.76 ± 0.01	Syn
PFOA + MMC + FURA	3.507 (2.11–4.90)	1.515 (1.06–2.85)	0.933	0.49 ± 0.02	Syn	0.87 ± 0.03	Syn	1.53 ± 0.12	Ant
PFOS + Hg + Cd	34.06 (21.13–45.38)	2.530 (1.32–3.05)	0.927	4.33 ± 0.18	Ant	3.39 ± 0.08	Ant	2.72 ± 0.12	Ant
PFOS + 2,4-D + PPB	13.58 (6.77–17.56)	3.908 (2.78–4.79)	0.921	2.32 ± 0.04	Ant	1.48 ± 0.02	Ant	0.97 ± 0.01	Add
PFOS + MMC + FURA	3.562 (1.50–6.04)	1.987 (0.75–2.34)	0.933	0.50 ± 0.05	Syn	0.55 ± 0.02	Syn	0.63 ± 0.02	Syn
% of Synergistic mixtures					50%		50%		50%
Multicomponent mixtures									
Mix 6	1.745 (1.60–2.62)	2.063 (1.49–2.95)	0.940	0.62 ± 0.01	Syn	0.75 ± 0.01	Syn	0.91 ± 0.02	Add
PFOA + Mix 6	2.859 (2.13–3.79)	1.585 (1.05–2.23)	0.935	0.45 ± 0.01	Syn	0.74 ± 0.05	Syn	1.22 ± 0.27	Add
PFOS + Mix 6	3.848 (3.05–4.56)	1.801 (1.12–2.34)	0.920	0.57 ± 0.01	Syn	0.75 ± 0.01	Syn	1.00 ± 0.04	Add
PFOA + PFOS + Mix 6	5.263 (5.59–8.81)	1.829 (1.20–2.46)	0.940	0.66 ± 0.01	Syn	0.85 ± 0.01	Syn	1.11 ± 0.03	Add
% of Synergistic mixtures					100%		100%		0%

Hg = Hg^{2+}, Cd = Cd^{2+}, PPB = propylparaben, 2,4-D = (2,4-dichlorophenoxy) acetic acid, FURA = furazolidone, MMC = mitomycin C, PFOA = perfluorooctanoic acid, and PFOS = perfluorooctane sulfonic acid. The parameters m, D_m and r are the slope and the linear correlation coefficient of the median-effect plot, which signifies the shape of the dose–effect curve, the potency (EC_{50}), and conformity of the data to the mass-action law, respectively [20,21]. CI < 1, CI = 1, and CI > 1 indicate synergism (Syn), additive effect (Add), and antagonism (Ant), respectively. EC_{10}, EC_{50} and EC_{90}, are the doses required to inhibit bioluminescence 10%, 50% and 90%, respectively.
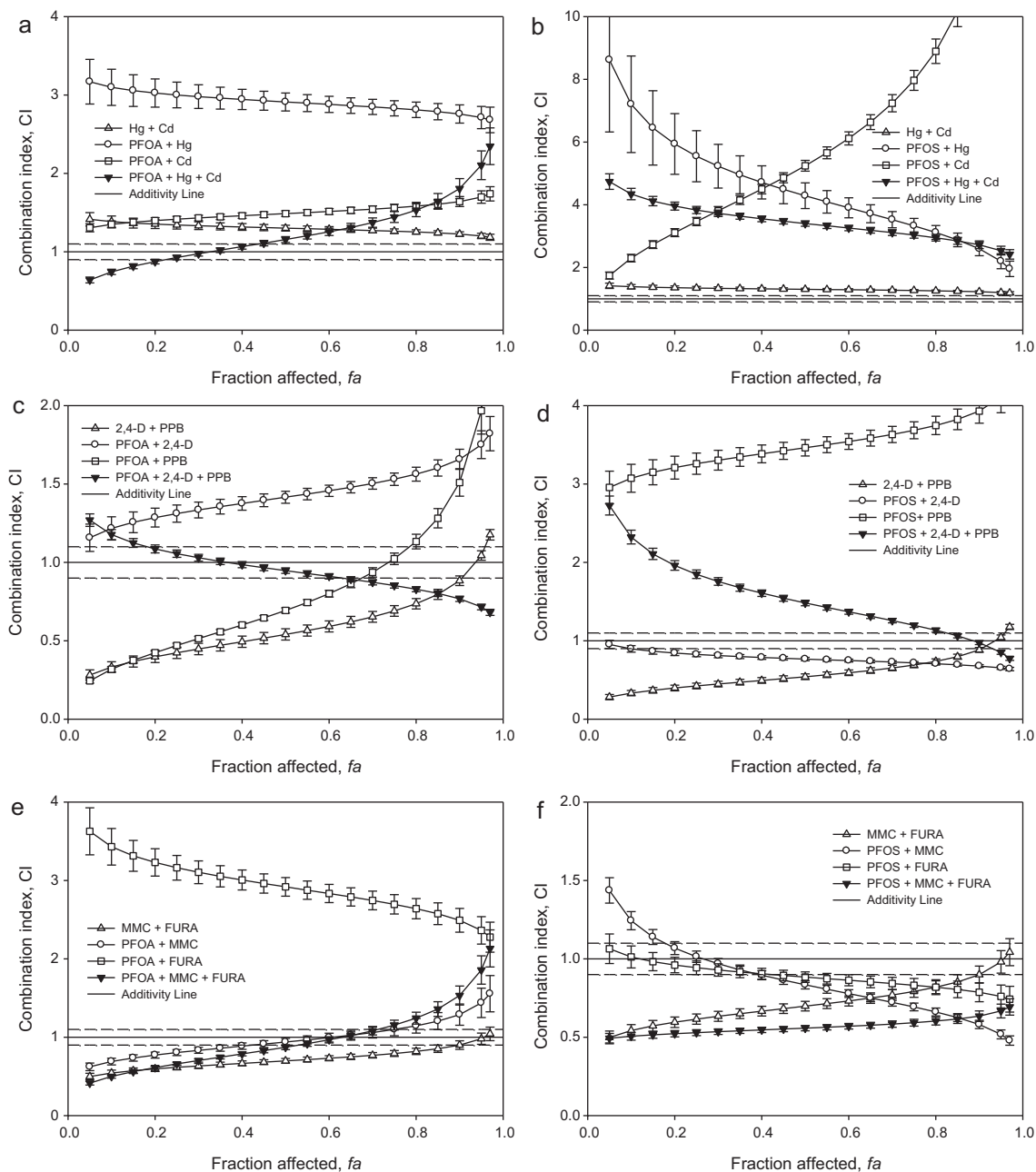
Fig. 1. Combination index plot (f_a–CI plot) for binary and ternary mixtures PFOA and PFOS with selected pollutants for the *Anabaena* CPB4337 test. CI values are plotted as a function of the fractional inhibition of bioluminescence (f_a) by computer simulation (CompuSyn) from $f_a = 0.10$ to 0.95. CI < 1, =1 and >1 indicates synergism, additive effect and antagonism, respectively. The vertical bars indicate 95% confidence intervals for CI values based on SDA (sequential deletion analysis) [21]. Broken lines indicate upper and lower limits of additivity [22]. Hg = Hg^{2+}, Cd = Cd^{2+}, PPB = propylparaben, 2,4-D = (2,4-dichlorophenoxy) acetic acid, FURA = furazolidone, MMC = mitomycin C.

a tendency toward additive effect. The ternary mixture of PFOS + Hg^{2+} + Cd^{2+} was clearly antagonistic in the whole range of f_a values meaning that the presence of PFOS significantly increased the observed antagonism of the binary Hg^{2+} + Cd^{2+} mixture. The highest correlation coefficients were those of the PFOS + Hg combination ($r = 0.995$) and Hg + Cd combination ($r = 0.994$), suggesting them as predominant in the three-component mixture (Table 3).

In the PFOA–biocides mixtures (Fig. 1c), the binary mixture of 2,4-D + PPB was synergistic at f_a levels below 0.75 and became additive at f_a values above this value. The binary combinations of PFOA + 2,4-D was increasingly antagonistic in the whole f_a range. The binary mixtures of PFOA + PPB led to a dual synergistic/antagonistic behavior: it was synergistic at f_a levels below

0.7, additive at f_a levels between 0.7 and 0.8 and it turned into an increasing antagonism at f_a levels below 0.8. The ternary PFOA + 2,4-D + PPB mixture also led to dual antagonistic/synergistic behavior being antagonistic at f_a values below 0.1, additive at f_a values between 0.1 and 0.7 and turning into synergistic at f_a values above 0.7; just the opposite of the observed behavior of the binary PFOA + PPB combination. In this case, all the correlation coefficients were negative, indicating an inverse relationship between the pattern of the interaction of the ternary mixture with respect to any of the binary combinations.

In the PFOS and biocides mixtures (Fig. 1d), the binary combination of PFOS + 2,4-D was synergistic in practically the whole range of f_a values and the binary combination PFOS + PPB was strongly antagonistic (CI > 3) in the whole range

Table 3
Correlation analyses between CI values of PFOA and PFOS ternary and multicomponent combinations (y) and their binary and ternary combinations (x) for *Anabaena* CPB4337 test.

Combinations			Regression parameters		
			x_0	m	r
Ternary combinations					
PFOA + Hg + Cd	vs	Hg + Cd	10.655	−7.240	− 0.969
	vs	PFOA + Hg	11.059	−3.369	− 0.957
	vs	PFOA + Cd	−4.583	3.893	0.988
PFOS + Hg + Cd	vs	Hg + Cd	−9.537	9.981	0.994
	vs	PFOS + Hg	1.855	0.349	0.995
	vs	PFOS + Cd	4.169	−0.111	− 0.878
PFOA + 2,4-D + PPB	vs	2,4-D + PPB	1.316	−0.618	− 0.947
	vs	PFOA + 2,4-D	2.189	−0.861	− 0.980
	vs	PFOA + PPB	1.162	−0.249	− 0.907
PFOS + 2,4-D + PPB	vs	2,4-D + PPB	2.683	−1.936	− 0.907
	vs	PFOS + 2,4-D	−3.202	6.142	0.998
	vs	PFOS + PPB	6.479	−1.409	− 0.950
PFOA + MMC + FURA	vs	MMC + FURA	−1.266	3.122	0.990
	vs	PFOA + MMC	−0.816	1.829	0.994
	vs	PFOA + FURA	4.514	−1.211	− 0.946
PFOS + MMC + FURA	vs	MMC + FURA	0.302	0.368	0.998
	vs	PFOS + MMC	0.739	−0.199	− 0.928
	vs	PFOS + FURA	1.101	−0.601	−0.956
Multicomponent combinations					
Mix 6	vs	Hg + Cd	1.587	−0.608	−0.995
	vs	2,4-D + PPB	0.705	0.153	0.985
	vs	MMC + FURA	0.612	0.255	0.997
PFOA + Mix 6	vs	PFOA + Hg +Cd	0.211	0.423	0.998
	vs	PFOA + 2,4-D + PPB	1.879	−1.198	−0.966
	vs	PFOA + MMC + FURA	0.329	0.419	0.999
PFOS + Mix 6	vs	PFOS + Hg +Cd	1.638	−0.268	−0.953
	vs	PFOS + 2,4-D + PPB	1.200	−0.313	−0.927
	vs	PFOS + MMC + FURA	−1.105	3.210	0.999
PFOA + PFOS + Mix 6	vs	PFOA + Hg +Cd	0.479	0.435	0.998
	vs	PFOA + 2,4-D + PPB	2.196	−1.234	0.967
	vs	PFOA + MMC + FURA	0.601	0.430	0.994
	vs	PFOS + Hg +Cd	2.089	−0.310	0.958
	vs	PFOS + 2,4-D + PPB	1.583	−0.363	0.934
	vs	PFOS + MMC + FURA	−1.074	3.693	0.999

Hg = Hg^{2+}, Cd = Cd^{2+}, PPB = propylparaben, 2,4-D = (2,4-dichlorophenoxy) acetic acid, FURA = furazolidone, MMC = mitomycin C, PFOA = perfluorooctanoic acid, and PFOS = perfluorooctane sulfonic acid. The parameters of linear regression equations: x_0 (value of y when $x = 0$); m (slope) and r (correlation coefficient) with all p-values <0.05.

of f_a values. The ternary combination PFOS + 2,4-D + PPB led to a dual antagonistic/synergistic behavior, similar to that found for the PFOA + 2,4-D + PPB mixture (Fig. 1c) but being antagonistic in practically the whole range of f_a values and only becoming synergistic at the highest f_a values (above 0.97). The highest correlation coefficient was found for the PFOS + 2,4-D combination ($r = 0.998$), suggesting that this combination interaction predominated in the three-component mixture (Table 3).

In the PFOA–pharmaceuticals mixtures (Fig. 1e), the binary mixture of FURA + MMC was synergistic in practically the whole range of f_a values, becoming nearly additive at f_a values close to 1. The binary combination PFOA + FURA was strongly antagonistic in the whole f_a range while the binary mixture of PFOA + MMC showed a dual synergistic/antagonistic behavior, synergistic at low to mean f_a values ($f_a < 0.5$), additive at f_a values between 0.45 and 0.7, and slightly antagonistic at f_a values above 0.7. The ternary mixture PFOA + FURA + MMC also showed a dual synergistic/antagonistic behavior, being synergistic at f_a values below 0.5, additive at f_a values between 0.5 and 0.7 and turning into antagonism at f_a values above 0.7. As expected, the highest correlation coefficient was found for the PFOA + MMC combination ($r = 0.994$), suggesting that this combination interaction predominated in the three-component mixture (Table 3).

In the PFOS–pharmaceuticals mixtures (Fig. 1f), both binary mixtures of PFOS + MMC and PFOS + FURA led to a dual antagonistic/synergistic behavior being antagonistic at f_a values below 0.2, additive at f_a values between 0.2 and 0.45 and dominated by synergism at f_a values above 0.45; however, although the interaction pattern for both binary mixtures was similar, the PFOS + MMC mixture showed a higher synergism at low f_a values and higher antagonism at the higher f_a levels. The ternary PFOS + MMC + FURA mixture was synergistic in practically the whole range of f_a values being more synergistic than any of the corresponding binary mixtures. The highest correlation coefficient was found for the MMC + FURA combination ($r = 0.988$), suggesting that this combination interaction clearly influenced the pattern of the observed interaction in the three-component mixture.

Fig. 2 shows a polygonogram of eight components which summarizes the evolution of the interactions of PFOA and PFOS with the six selected pollutants in binary mixtures at three representative levels of effect ($f_a = 0.1$, 0.5 and 0.9). Quantitative values of CI at this f_a levels can be seen in Table 2. The polygonogram (Fig. 2) clearly shows that the pattern of the interactions in binary mixtures is globally dominated by antagonistic interactions of the perfluorinated surfactants with the different pollutants particularly at the highest levels of effect; the exception to this were the interactions
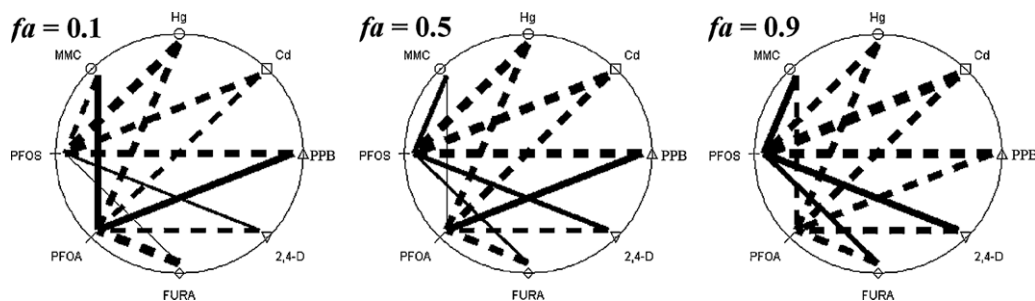
Fig. 2. Polygonograms showing the toxicological interactions of PFOA and PFOS with selected pollutants in their binary combinations for the *Anabaena* CPB4337 test at three representative effect levels: $f_a = 0.1$, $f_a = 0.5$, $f_a = 0.9$. Solid lines indicate synergism, broken lines indicate antagonism. The thickness of the line represents the strength of synergism or antagonism. Hg = Hg^{2+}, Cd = Cd^{2+}, PPB = propylparaben, 2,4-D = (2,4-dichlorophenoxy) acetic acid, FURA = furazolidone, MMC = mitomycin C.

of PFOS with the herbicide 2,4-D and with the antibacterial furazolidone which were synergistic along all the representative f_a levels, and the synergistic interactions of PFOA with MMC and PPB at low to mean effect levels.

3.3. Toxicological interactions of PFOA and PFOS in multicomponent mixtures with selected pollutants in the Anabaena CPB4337 bioluminescence test

In order to evaluate any antagonistic or synergistic effect between PFOA and/or PFOS and complex mixtures of the selected pollutants, we made 4 different multicomponent mixtures: a mixture of 6 components which includes the selected pollutants previously used (Hg^{2+}, Cd^{2+}, PPB, 2,4-D, MMC and FURA), named Mix 6; 2 mixtures of 7 components in which we analyzed the effect of the addition of PFOS or PFOA to the complex mixture Mix 6: PFOA + Mix 6 and PFOS + Mix 6, and an 8 component mixture including both PFOA and PFOS and the 6 selected pollutants, named PFOA + PFOS + Mix 6; together with this multicomponent mixture, we also assayed the binary mixture PFOA + PFOS, which allowed us to check the combined effect of the two perfluorinated surfactants on the mixture behavior.

Fig. 3 shows the f_a–CI plots for the binary mixture PFOA + PFOS (Fig. 3a), as well as those of the different multicomponent mixtures Mix 6, PFOA + Mix 6, PFOS + Mix 6 and PFOA + PFOS + Mix 6 (Fig. 3b). As shown in the figure, binary mixture of both perfluorinated surfactants PFOA + PFOS showed a strong antagonism in the whole range of f_a values. Regarding multicomponent mixtures (Fig. 3b), the multicomponent mixture Mix 6 was synergistic in the whole range of f_a values, keeping a constant CI value of around 0.7. The addition of PFOA or PFOS to mix 6 resulted in a dual effect on the f_a–CI behavior: at low to mean levels, both mixtures, PFOA + Mix 6 and PFOS + Mix 6 became more synergistic than Mix 6 with a decrease in the CI values down to 0.47 at very low effect levels ($f_a < 0.1$); however, at high f_a values (>0.8), both 7-component mixtures approached additivity. The addition of both PFOA and PFOS to the multicomponent mixture Mix 6 had a marked effect leading to a dual synergistic/antagonistic behavior; at the lowest f_a values, the mixtures was more synergistic than mix 6 but the synergism significantly decreased with increasing f_a levels until it approached an additive effect at f_a levels between 0.3 and 0.7 and turned into antagonism at f_a values > 0.7. Correlation analyses were also made between CI values of the 4 complex mixtures and their binary (for Mix 6) or ternary combinations (for PFOA + Mix 6 and PFOS + Mix 6) to determine which component mixture interactions were predominant in the multicomponent mixtures (Table 3).

For the Mix 6 mixture, the highest positive correlation coefficient was found for the binary mixture of the two pharmaceuticals MMC + FURA ($r = 0.997$) suggesting that this combination
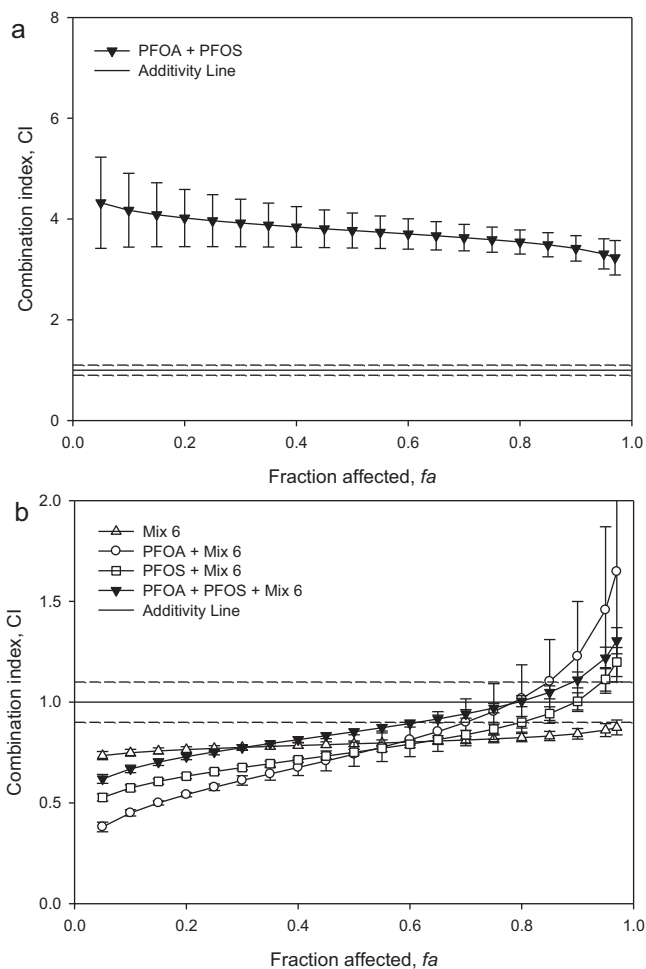

Fig. 3. Combination index plot (f_a–CI plot) for the binary mixture PFOA + PFOS (a), and multicomponent mixtures of PFOA and PFOS with selected pollutants (b) for the *Anabaena* CPB4337 test. CI < 1, =1 and >1 indicates synergism, additive effect and antagonism, respectively. The vertical bars indicate 95% confidence intervals for CI values based on SDA (sequential deletion analysis) [21]. Broken lines indicate upper and lower limits of additivity [22]. Mix 6 = Hg^{2+}, Cd^{2+}, PPB, 2,4-D, FURA, MMC.

interaction predominated in this mixture. In both the PFOA + Mix 6 and PFOS + Mix 6 combinations, the ternary mixtures including pharmaceuticals (PFOA + MMC + FURA and PFOS + MMC + FURA) showed the highest correlation coefficients ($r = 0.999$ for both mixtures); besides, for the PFOA + Mix 6 combination, the ternary PFOA + heavy metals mixture also showed a positive high correlation coefficient ($r = 0.998$). In the most complex mixture which

Table 4
Observed toxicities of the multicomponent mixtures Mix 6, PFOA + Mix 6, PFOS + Mix 6 and PFOA + PFOS + Mix 6 and combination index (CI) calculations at mixture NOECs concentrations.

Mixture	Total mixture concentration[a] (mg/l)	Observed toxicity (% inhibition)	Experimental CI values
Mix 6	0.664	17.91 ± 5.02	0.66 ± 0.04
PFOA + Mix 6	1.210	23.16 ± 9.65	0.54 ± 0.06
PFOS + Mix 6	1.835	19.09 ± 5.03	0.63 ± 0.02
PFOA + PFOS + Mix 6	2.382	21.40 ± 8.03	0.73 ± 0.04

[a] Total mixture concentrations at mixture NOECs as estimated by Dunnett's test [23,24]. The individual concentrations (mg/l) of each component at mixture NOECs were as follows: $Hg^{2+} = 7.81 \times 10^{-4}$, $Cd^{2+} = 0.0031$, PPB = 0.426, 2,4-D = 0.3905, MMC = 0.0011, FURA = 0.033, PFOA = 0.5464, PFOS = 1.171.

included both perfluorinated surfactants and all the selected pollutants (PFOA + PFOS + Mix 6), the highest correlation coefficient was found for the ternary PFOS + MMC + FURA and PFOA + Hg + Cd mixtures ($r = 0.999$ and 0.998, respectively), closely followed by PFOA + MMC + FURA ($r = 0.994$), indicating that the mixtures including these two pharmaceuticals followed by those containing both heavy metals clearly influenced the observed interaction behavior of the four complex mixtures.

Synergism is predicted by the CI method at low to very low effect levels in the complex mixtures tested (Fig. 3b), this might have implications in risk assessment; thus, in order to find out whether these predicted CIs could be real, we made a set of experiments in which, for the four complex mixtures, chemicals were mixed at their calculated mixture NOECs concentrations. At these concentrations, individual components of complex mixtures did not exert any toxicity (not shown). The results on observed toxicity and calculated CI values for the four mixtures are shown in Table 4. All these mixtures inhibited luminescence by around 20% ($f_a = 0.2$), the computed CI values for these levels of effect for each mixture clearly indicated synergism (CI in the range from 0.54 to 0.73), confirming the predicted synergism at low/very low effect levels.

4. Discussion

In this work, we describe by the first time the toxicological interactions of two of the most environmentally relevant fluorinated surfactants, PFOS and PFOA [4,5] with several priority and emerging pollutants in a bioluminescent cyanobacterium which has previously proved very useful in ecotoxicity studies [8,9,16,17].

As shown in Fig. 2 the interaction of PFOA and PFOS with organics exhibited a clearly different pattern. PFOS displayed synergistic interactions with 2,4-D, FURA and MMC for almost all f_a levels; whereas, except for PPB, antagonistic interactions globally dominated mixtures with PFOA. This fact might be related to the role of PFOS in enhancing the accessibility and cell uptake of co-existing hydrophobic compounds as suggested by Liu et al. [15].

The chemicals we have used have different hydrophobicity as shown by their $\log D_{ow}$ values shown in Table 1. According to these values, PPB and PFOA are the most hydrophobic and PFOS and 2,4-D the most polar of the organic compounds; the polar surface area (Table 1) gives an idea of the ability of a particular chemical to permeate cell membranes since it is a descriptor that was shown to correlate well with passive molecular transport through membranes [19]. PFOA has a lower polar surface area than PFOS, perhaps indicating a higher capability of permeating membranes; in fact, Nobels et al. [27] reported a higher level of membrane damage by PFOA than that induced by PFOS. Our results show that PFOA interacted synergistically with the most hydrophobic compound PPB and antagonistically with the most polar one, 2,4-D, in their binaries while PFOS interacted just in the opposite way with both chemicals.

Our results suggest, however, a more complex behavior because PFOS and PFOA interacted in opposite ways with co-existing compounds with similar hydrophobicity such as MMC and FURA. These results point toward a more complex mechanism of interaction of PFOA and PFOS with organics not directly related with their relative hydrophobicity. Several authors have already suggested that the toxicity of PFOS and PFOA should be addressed separately as they seem to behave differently, independently of the toxicity endpoint [27–29].

The interaction of both PFOS and PFOA with heavy metals was totally different to the ones with the organic chemicals; in the case of Hg and Cd, both PFCs interacted mostly antagonistically; the most plausible explanation could be the stabilization of the metals through either complexation [30–32] or counter-ion exchange with the negatively charged surfactants at the assay pH as proposed for the reduction of Cd and Pb uptake in a macroalga in the presence of the anionic surfactant SDS [33].

With regards to complex mixtures, the mixture of the six compounds was clearly synergistic at almost all effect levels, addition of PFOA or PFOS increased the synergism, particularly at low effect levels, with the most hydrophobic PFC, PFOA, inducing a higher synergistic interaction; as expected due to their antagonistic behavior in their binary, the addition of both PFOA and PFOS to mix 6 decreased the observed synergistic interaction in practically the whole f_a range, indicating that the presence of both PFCs could decrease the toxicity of co-existing chemicals.

The predicted synergism at low to very low effect levels in all the complex mixtures indicated a potential toxicological risk associated with the co-existence of these compounds at low or very low concentrations in the aquatic environment; to demonstrate that the predicted synergism by CI was real of each mixture, we tested the individual toxicity of each compound at the concentration present in these mixtures, and we found no toxic effect. Them we made new mixtures based on these concentrations, finding a luminescence inhibition of around 20% with experimental CIs smaller than 1, indicating that the predicted synergism by the CI method was real and could be of environmental relevance.

As different PFCs may co-exist in the same environment and toxicological interactions among them as the ones showed in this report could occur, studies of the combined toxicities between as many PFCs as possible as well as between them and other substances should be performed, specially directed to find out compounds with might interact non-additively or which may greatly influence the pattern of interactions in complex mixtures. We propose that the CI method which quantifies the interactions, if any, and which is independent of the mechanism of action of the tested compounds may be a useful approach to carry out such studies.

5. Conclusions

When individual toxicities were tested, the perfluorinated surfactants PFOS and PFOA, 2,4-D and propylparaben showed lower toxicity than Hg^{2+}, Cd^{2+}, mitomycin C and furazolidone which could be considered as "very toxic to aquatic life". The antagonistic interaction between PFOA and PFOS at all effect levels as well as the relative hydrophobicity of the tested compounds could explain the opposite interaction pattern of both perfluorinated surfactants with the organic chemicals. Both PFOA and PFOS interacted antagonistically with both heavy metals; this could be explained by stabilization of the cations in the solution by the negatively charged surfactants. The CI method predicted synergism in all the complex mixtures at low effect levels which may have implications in the real environment; pollutant combinations at their mixture NOECs confirmed the predicted synergism.

Acknowledgements

References

[1] S.A. Beach, J.L. Newsted, K. Coady, J.P. Giesy, Ecotoxicological evaluation of perfluorooctanesulfonate (PFOS), Rev. Environ. Contam. Toxicol. 186 (2006) 133–174.

[2] OECD, Results of the 2006 survey on production and use of PFOS, PFAS, PFOA, PFCA, their related substances and products/mixtures containing these substances, in: p.a.b. (Ed.), Environment Directorate Joint Meeting of the Chemicals Committee and the Working Party on Chemicals, 2006.

[3] R. Rosal, A. Rodriguez, J.A. Perdigon-Melon, A. Petre, E. Garcia-Calvo, M.J. Gomez, A. Aguera, A.R. Fernandez-Alba, Occurrence of emerging pollutants in urban wastewater and their removal through biological treatment followed by ozonation, Water Res. 44 (2010) 578–588.

[4] R. Loos, G. Locoro, S. Comero, S. Contini, D. Schwesig, F. Werres, P. Balsaa, O. Gans, S. Weiss, L. Blaha, M. Bolchi, B.M. Gawlik, Pan-European survey on the occurrence of selected polar organic persistent pollutants in ground water, Water Res. 44 (2010) 4115–4126.

[5] K.E. Murray, S.M. Thomas, A.A. Bodour, Prioritizing research for trace pollutants and emerging contaminants in the freshwater environment, Environ. Pollut. 158 (2010) 3462–3471.

[6] V.T. Nguyen, M. Reinhard, G.Y. Karina, Occurrence and source characterization of perfluorochemicals in an urban watershed, Chemosphere 82 (2011) 1277–1285.

[7] M. Cleuvers, Aquatic ecotoxicity of pharmaceuticals including the assessment of combination effects, Toxicol. Lett. 142 (2003) 185–194.

[8] I. Rodea-Palomares, A.L. Petre, K. Boltes, F. Leganes, J.A. Perdigon-Melon, R. Rosal, F. Fernandez-Pinas, Application of the combination index (CI)-isobologram equation to study the toxicological interactions of lipid regulators in two aquatic bioluminescent organisms, Water Res. 44 (2010) 427–438.

[9] R. Rosal, I. Rodea-Palomares, K. Boltes, F. Fernandez-Pinas, F. Leganes, A. Petre, Ecotoxicological assessment of surfactants in the aquatic environment: combined toxicity of docusate sodium with chlorinated pollutants, Chemosphere 81 (2010) 288–293.

[10] L.K. Teuschler, Deciding which chemical mixtures risk assessment methods work best for what mixtures, Toxicol. Appl. Pharmacol. 223 (2007) 139–147.

[11] S.D. Haigh, A review of the interaction of surfactants with organic contaminants in soil, Sci. Total Environ. 185 (1996) 161–170.

[12] W. Hu, P.D. Jones, W. DeCoen, L. King, P. Fraker, J. Newsted, J.P. Giesy, Alterations in cell membrane properties caused by perfluorinated compounds, Comp. Biochem. Physiol. C: Toxicol. Pharmacol. 135 (2003) 77–88.

[13] S. Jernbro, P.S. Rocha, S. Keiter, D. Skutlarek, H. Farber, P.D. Jones, J.P. Giesy, H. Hollert, M. Engwall, Perfluorooctane sulfonate increases the genotoxicity of cyclophosphamide in the micronucleus assay with V79 cells. Further proof of alterations in cell membrane properties caused by PFOS, Environ. Sci. Pollut. Res. Int. 14 (2007) 85–87.

[14] S. Kim, K. Ji, S. Lee, J. Lee, J. Kim, S. Kim, Y. Kho, K. Choi, Perfluorooctane sulfonic acid exposure increases cadmium toxicity in early life stage of zebrafish, *Danio rerio*, Environ. Toxicol. Chem. 30 (2010) 870–877.

[15] W. Liu, Y.B. Zhang, X. Quan, Y.H. Jin, S. Chen, Effect of perfluorooctane sulfonate on toxicity and cell uptake of other compounds with different hydrophobicity in green alga, Chemosphere 75 (2009) 405–409.

[16] I. Rodea-Palomares, F. Fernández-Piñas, C. González-García, F. Leganés, Use of lux-marked cyanobacterial bioreporters for assessment of individual and combined toxicities of metals in aqueous samples, in: Handbook on Cyanobacteria: Biochemistry, Biotechnology and Applications, Nova Science Publishers, Inc., New York, USA, 2009.

[17] I. Rodea-Palomares, C. Gonzalez-Garcia, F. Leganes, F. Fernandez-Pinas, Effect of pH, EDTA, and anions on heavy metal toxicity toward a bioluminescent cyanobacterial bioreporter, Arch. Environ. Contam. Toxicol. 57 (2009) 477–487.

[18] J.A. Sohm, E.A. Webb, D.G. Capone, Emerging patterns of marine nitrogen fixation, Nat. Rev. Microbiol. 9 (2011) 499–508.

[19] P. Ertl, B. Rohde, P. Selzer, Fast calculation of molecular polar surface area as a sum of fragment-based contributions and its application to the prediction of drug transport properties, J. Med. Chem. 43 (2000) 3714–3717.

[20] R. Rosal, I. Rodea-Palomares, K. Boltes, F. Fernandez-Pinas, F. Leganes, S. Gonzalo, A. Petre, Ecotoxicity assessment of lipid regulators in water and biologically treated wastewater using three aquatic organism, Environ. Sci. Pollut. Res. 17 (2009) 135–144.

[21] OECD, Guidelines for the Testing of Chemicals, No. 23: Guidance Document on Aquatic Toxicity Testing of Difficult Substances and Mixtures, 2000, PDF Edition, 10 May 2002, p 53, ISBN: 9789264078406.

[22] T.C. Chou, P. Talalay, Quantitative analysis of dose–effect relationships: the combined effects of multiple drugs or enzyme inhibitors, Adv. Enzyme Regul. 22 (1984) 27–55.

[23] T.C. Chou, Theoretical basis, experimental design, and computerized simulation of synergism and antagonism in drug combination studies, Pharmacol. Rev. 58 (2006) 621–681.

[24] T.C. Chou, N. Martin, CompuSyn for Drug Combinations: PC Software and User's Guide: A Computer Program for Quantification of Synergism and Antagonism in Drug Combinations and the Determination of IC50 and ED50 and LD50 Values, ComboSyn, Inc., Paramus, NJ, 2005.

[25] U.S. EPA, Short-Term Methods for Estimating the Chronic Toxicity of Effluents and Receiving Waters to Freshwaters Organism, U.S. Environmental Protection Agency, 1994.

[26] U.S. EPA, Methods for Measuring the Acute Toxicity of Effluents and Receiving Waters to Freshwater and Marine Organism, United States Environmental Protection Agency, 2002.

[27] I. Nobels, F. Dardenne, W. De Coen, R. Blust, Application of a multiple endpoint bacterial reporter assay to evaluate toxicological relevant endpoints of perfluorinated compounds with different functional groups and varying chain length, Toxicol In Vitro 24 (2010) 1768–1774.

[28] L.W. Yeung, K.S. Guruge, N. Yamanaka, S. Miyazaki, P.K. Lam, Differential expression of chicken hepatic genes responsive to PFOA and PFOS, Toxicology 237 (2007) 111–125.

[29] L.W. Yeung, E.I. Loi, V.Y. Wong, K.S. Guruge, N. Yamanaka, N. Tanimura, J. Hasegawa, N. Yamashita, S. Miyazaki, P.K. Lam, Biochemical responses and accumulation properties of long-chain perfluorinated compounds (PFOS/PFDA/PFOA) in juvenile chickens (*Gallus gallus*), Arch. Environ. Contam. Toxicol. 57 (2009) 377–386.

[30] C.D. Campbell, M. Hird, D.G. Lumsdon, J.C. Meeussen, The effect of EDTA and fulvic acid on Cd, Zn, and Cu toxicity to a bioluminescent construct (pUCD607) of *Escherichia coli*, Chemosphere 40 (2000) 319–325.

[31] A. Kungolos, P. Samaras, V. Tsiridis, M. Petala, G. Sakellaropoulos, Bioavailability and toxicity of heavy metals in the presence of natural organic matter, J. Environ. Sci. Health Part A Tox. Hazard. Subst. Environ. Eng. 41 (2006) 1509–1517.

[32] V. Tsiridis, M. Petala, P. Samaras, S. Hadjispyrou, G. Sakellaropoulos, A. Kungolos, Interactive toxic effects of heavy metals and humic acids on *Vibrio fischeri*, Ecotoxicol. Environ. Saf. 63 (2006) 158–167.

[33] K. Masakorala, A. Turner, M.T. Brown, Influence of synthetic surfactants on the uptake of Pd, Cd and Pb by the marine macroalga, *Ulva lactuca*, Environ. Pollut. 156 (2008) 897–904.